Biophysical Journal Volume 71 November 1996 2645–2655

Distance Between CYS-201 in Erythrocyte Band 3 and the Bilayer Measured by Single-Photon Radioluminescence

Bernard J.-M. Thevenin,* Stephen E. Bicknese,*# A. S. Verkman,# and Stephen B. Shohet*
Departments of *Laboratory Medicine and of #Medicine and Physiology, Cardiovascular Research Institute, University of California, San Francisco, California 94143 USA

ABSTRACT Single-photon radioluminescence (SPR), the excitation of fluorophores by short-range β-decay electrons, was developed for the measurement of submicroscopic distances. The cytoplasmic domain of band 3 (cdb3) is the primary, multisite anchorage for the erythrocyte skeleton. To begin to define the membrane arrangement of the highly asymmetrical cdb3 structure, the distance from the bilayer of Cys-201 next to the "hinge" of cdb3 was measured by both SPR and resonance energy transfer (RET). cdb3 was labeled at Cys-201 with fluorescein maleimide. For SPR measurements, the bilayer was labeled with [^{3}H]oleic acid. The corrected cdb3-specific SPR signal was 98 $\pm$ 2 cps μCi^{-1} [μmol band 3]$^{-1}$. From this and the signal from a parallel sample in which ^3H_2O was substituted for [^{3}H]oleic acid to create uniform geometry between ^{3}H and the fluorophores, a Cys-201-to-bilayer separation of 39 $\pm$ 7 Å was calculated. Confirmatory distances of 40 and 43 Å were obtained by RET between fluorescein on Cys-201 and eosin and rhodamine B lipid probes, respectively. This distance indicates that Cys-201 lies near band 3's vertical axis of symmetry and that the subdomain of cdb3 between the hinge and the membrane is not significantly extended. In addition, these results validate SPR as a measure of molecular distances in biological systems.

INTRODUCTION

Band 3 is the principal component of the erythrocyte membrane and exists in situ as a mixture of dimers and tetramers (for reviews see Jennings, 1989; Tanner, 1993; Reithmeier, 1993). Each band 3 molecule is composed of two structural units: a 55-kDa membrane multispanning domain and a 43-kDa cytoplasmic domain connected by a flexible, easily proteolyzed segment. The major function of the membrane domain is to carry out the rapid exchange of HCO_3^- for Cl^- anions across the bilayer, a process that is blocked by stoichiometric labeling with disulfonate stilbenes (DS). The major function of the cytoplasmic domain of band 3 (cdb3) is to connect the spectrin-based skeleton with the membrane, primarily via its association with ankyrin, and secondarily via its interaction with band 4.1 and band 4.2 (for a review, see Low, 1986). Interactions of band 3 with the cytoskeleton are critical to cell morphology, deformability, and stability (Agre et al., 1981; Peters and Lux, 1993; Low et al., 1991). Although the primary sequence of band 3 is known (Tanner et al., 1988), and a 20-Å resolution map of the membrane domain has been obtained (Wang et al., 1994), the structure of cdb3 is not clearly defined. After proteolytic release from the membrane, cdb3 is isolated as a dimer exhibiting hydrodynamic properties suggestive of a highly asymmetrical structure that could extend up to 250 Å (Low, 1986). Indeed, wormlike extensions beneath the bilayer ascribed to cdb3 have been observed in electron micrographs (Weinstein et al., 1978). An open flexible region, or "hinge," near the middle of the cdb3 sequence is believed to serve as a pivotal region for the bending of the molecule that is associated with changes in pH (Low et al., 1984) and probably with other conformational changes observed under physiological conditions (Salhany and Cassoly, 1989; Thevenin et al., 1994).

Multiple orientations of cdb3 with respect to the bilayer are possible, given its flexible connection to the membrane domain and its high asymmetry. For example, as depicted in Fig. 1, cdb3 could extend either vertically from or parallel to the bilayer. An orientation of cdb3 parallel to the bilayer would place the cytoskeleton attachment sites closer to the membrane and create much greater cytoskeleton-bilayer intimacy than a vertical orientation. This orientation of cdb3 is important because it is the primary site of cytoskeleton: membrane interactions that are responsible for critical mechano-physical properties of the erythrocyte membrane. Moreover, the membrane conformation of cdb3 appears to regulate the association of band 3 with ankyrin and thus with the cytoskeleton (Thevenin and Low, 1990). Using resonance energy transfer (RET), Rao et al. (1979) have measured a separation of ~40 Å between the DS-binding sites and a cluster of four cytoplasmic cysteines in the band 3 dimer (Cys-cluster) (Thevenin et al., 1989). However, this single distance is insufficient to infer the position of the cysteines and the orientation of cdb3 in relation to the bilayer. Determination of the distance between the plane of the bilayer and the Cys-cluster that includes Cys-201 next to the hinge would be helpful in beginning to define the arrangement of cdb3 in the membrane.

RET has been extensively used to measure molecular distances in biological systems (Wu and Brand, 1994). However, because RET depends on the inverse sixth power of the distance between donor and acceptor fluorophores, it

Received for publication 29 April 1996 and in final form 30 July 1996.

Address reprint requests to Dr. Bernard Thevenin, Box 0134, University of California, San Francisco, CA 94143-0134. Tel.: 415-476-3931; Fax: 415-476-9625; bt7in@itsa.ucsf.edu.

0006-3495/96/11/2645/11 $2.00

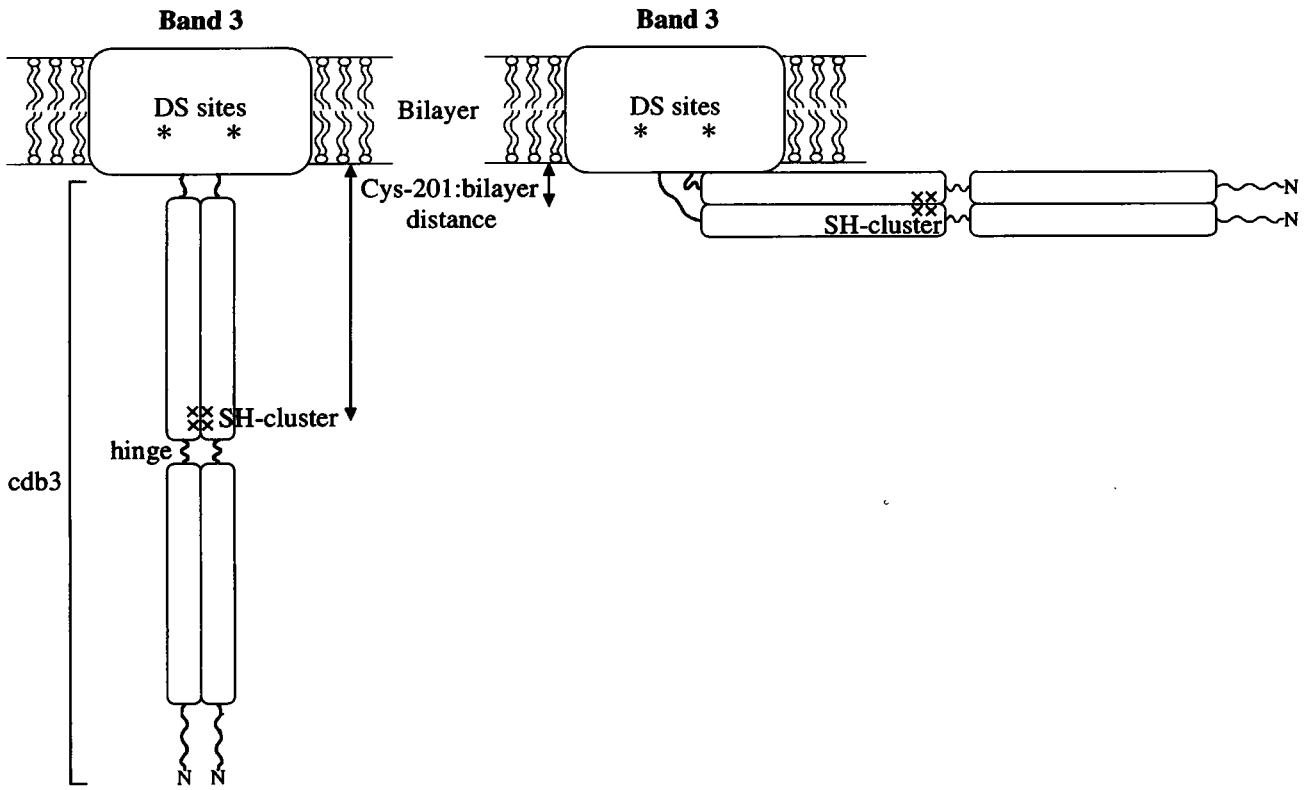

FIGURE 1 Schematic diagram of the band 3 dimer showing two extreme orientations for cdb3 in the membrane. Structural characteristics of band 3 are described in the text. On the right, the two regions near the hinge and the N-terminus that constitute the ankyrin association site for the cytoskeleton (Willardson et al., 1989) are apposed against the membrane, creating a high degree of physical intimacy of the skeletal network with the bilayer. On the left, these attachment sites are distant from the bilayer, decreasing the physical connection between the membrane and its supporting skeleton. The two DS sites and the four clustered cysteines of the dimer are shown, and the distance to be measured between Cys-201 and the bilayer is indicated for both situations.

is generally not suitable for measuring donor-acceptor separations exceeding 100 Å. To measure greater molecular distances, our laboratory has recently developed the technique of single-photon radioluminescence (SPR), in which the energy deposited by β-particles from a tritiated source excites nearby acceptor fluorophores (Bicknese et al., 1992). Because the energy deposited in the medium decreases approximately with the inverse square of the distance from the source, single-photon counting of the acceptor fluorescence is theoretically suitable for measuring molecular separations of up to ~1000 Å (Shahrohk et al., 1992; Bicknese et al., 1992). However, SPR has not yet been tested against the established RET technique, and its ability to reliably measure molecular distances in biological samples remains to be established.

The goal of the present study was to measure the separation between Cys-201 near the cytoplasmic hinge in band 3 and the surface of the bilayer by both SPR and RET. The distance between Cys-201 and the bilayer under physiological conditions measured by SPR (39 Å) was found to be very similar to that measured by RET (~41 Å), thus validating SPR for the measurement of molecular distances in intact biological systems. Furthermore, this distance indicates that the structure of cdb3 between the hinge and the membrane is not elongated.

MATERIALS AND METHODS

Labeling procedures

1 M KI-extracted inside-out-vesicles (KIOVs) were prepared from fresh normal erythrocytes as described (Bennett, 1983). Residue Cys-201 of cdb3 in KIOVs (2 mg/ml) was labeled with fluorescein as reported (Thevenin et al., 1994), except that the reaction was carried out with 50 μM fluorescein maleimide (Molecular Probes) in 5 mM NaH_2PO_4, 1 mM EDTA, 135 mM NaCl, pH 8 (buffer A). Fluorescein maleimide-labeled KIOVs (FM-KIOVs) were dialyzed extensively in 10 mM NaH_2PO_4, 1 mM EDTA, 127 mM NaCl, pH 7.4 (buffer B). A portion of the FM-KIOVs at 1 mg/ml in buffer A was cleaved with 6 μg/ml *Nα-p*-tosyl-L-lysine chloro-methyl ketone (TLCK)-treated chymotrypsin for 30 min at 0°C, diluted 33-fold in buffer B containing 0.5 mM diisopropyl fluorophosphate, and centrifuged to remove cdb3 fragments. After the removal of cdb3, chymotrypsin-cleaved FM-KIOVs (clv-FM-KIOVs) were then dialyzed against buffer B. Protein concentrations were determined according to the method of Lowry et al. (1951) after the samples were boiled in 5% SDS. Band 3 molar concentrations in uncleaved samples were calculated using a protein fraction of 0.5 for band 3 in KIOVs and M_r = 102,000. To compare samples of FM-KIOVs and clv-FM-KIOVs with the same membrane surface area, concentrations were determined as molar concentra-

tions of band 3 membrane domain. This was achieved by comparing Coomassie staining intensities of band 3 membrane domain from clv-FM-KIOVs unknowns and from known amounts of unwashed, chymotrypsin-cleaved FM-KIOVs. Fluorescein concentration was measured from sample absorbance in 0.1 M NaOH and 0.2% SDS (Beckmann DU-7 spectrophotometer), using ϵ_{max} = 86,000 M^{-1} cm^{-1} for fluorescein. Labeling stoichiometries of FM-KIOVs and clv-FM-KIOVs were 1.9 and 0.8 mol fluorescein/mole of band 3, respectively.

For RET measurements, the exposed cytoplasmic leaflet of the bilayer of FM-KIOVs or clv-FM-KIOVs was labeled with hexadecanoylaminoeosin (HAE) or octadecylrhodamine B (ORB) (Molecular Probes, Eugene, OR) 5 min before fluorescence measurements. One microliter of the desired dilution of the probe in ethanol was injected into a 1-ml sample containing 9.8 nM band 3 during vigorous stirring. For SPR measurements, the bilayer in samples containing 14.5 μM band 3 in buffer B was labeled with [9,10(n)-^{3}H]oleic acid (New England Nuclear; 10 Ci/mmol) by ethanol injection (2.3% v/v final ethanol concentration). In parallel samples, ^3H_2O diluted to 10 Ci/mmol in ethanol was injected in place of [^{3}H]oleic acid.

SPR measurements

Radioluminescence was measured using the improved instrumentation described by Bicknese et al. (1995). Glass vials containing aqueous samples with or without radiolabel and/or fluorescein label were placed within a mirrored ellipsoidal photon collection chamber adjacent to a cooled photomultiplier. A KV-470 cut-on filter was used to exclude short-wavelength intrinsic fluorescence in the sample (from tryptophans and tyrosines) and the majority of the *Bremsstrahlung* background signal (Bicknese et al., 1992). SPR samples consisted of FM-KIOVs or clv-FM-KIOVs, which were labeled with [^{3}H]oleic acid or to which ^3H_2O was added. In addition, samples consisting of nonfluorescent KIOVs labeled with [^{3}H]oleic acid were used to measure the *Bremsstrahlung* component of the SPR signal. All samples were prepared in triplicate and introduced into preweighed ~0.9-ml glass vials. The sample volume in each sealed vial was determined gravimetrically using a sample density of 1 g cm^{-3}. The vials were kept overnight in the dark at 4°C and then equilibrated at 17°C for SPR measurements. After measurement of radioluminescence signals, sample radioactivity was determined from scintillation spectrometry on quadruplicate 10-μl aliquots from each vial (Beckmann LS8000 scintillation counter).

Measured radioluminescence signals (average counts per second (cps) from six measurements of 120 s each) were background-corrected and normalized according to Eq. 1:

$$S_{bn} = (S_{rad} - S_{blk})/(R_S A_S), \quad (1)$$

where S_{bn} is the background-corrected, normalized SPR sample signal in cps μCi^{-1} [μmol band 3]$^{-1}$, S_{rad} is the SPR sample signal (cps), S_{blk} is the SPR sample blank signal (cps), R_S is the SPR sample radioactivity (μCi), and A_S is the sample amount (μmol band 3). Sample blanks consisted of parallel preparations labeled with nonradioactive oleic acid in place of [^{3}H]oleic acid. The background-corrected, normalized *Bremsstrahlung* signal, B_{bn}, was similarly calculated from B_{rad}, the SPR sample signal, B_{blk}, the *Bremsstrahlung* blank signal, R_B, the *Bremsstrahlung* sample radioactivity, and A_B, the *Bremsstrahlung* sample amount. The *Bremsstrahlung* signal was measured with nonfluorescent KIOV samples labeled with [^{3}H]oleic acid. The corrected SPR signal L_{cor} (in cps μCi^{-1} [μmol band 3]$^{-1}$) could then be obtained by correcting S_{bn} for inner-filter effect and subtracting the *Bremsstrahlung* component:

$$L_{cor} = (S_{bn} \cdot I_a) - B_{bn} = [I_a(S_{rad} - S_{blk})/(R_S A_S)] - [(B_{rad} - B_{blk})/(R_B A_B)], \quad (2)$$

where I_a is the inner-filter correction. I_a for a given sample was evaluated from Eq. 3 by summing over $\Delta\lambda$ = 1 nm intervals between 470 and 700 nm:

$$I_a = \sum[F_a(\lambda) \times 10^{+(\varepsilon_a(\lambda)\, l\, c_a)}\, \Delta\lambda]/\sum[F_a(\lambda)\, \Delta\lambda], \quad (3)$$

where λ is the wavelength (nm), $F_a(\lambda)$ is the uncorrected fluorescence of the acceptor fluorophores at λ, $\varepsilon_a(\lambda)$ is the molar absorbance of the acceptor at λ (M^{-1} cm^{-1}), c_a is the concentration of acceptor (M), and l = 0.497 cm is the average distance traveled by photons emitted within the sample vial before exiting the vial. The value of l was determined from computer modeling of photon paths for the cylindrical geometry of the vials.

A fraction of the total fluorescein label in FM-KIOVs was not bound to cdb3, yet it contributed to the radioluminescence signal from FM-KIOV samples. Because this fraction of fluorescein was that remaining after selective removal of labeled-cdb3, clv-FM-KIOVs were used to determine the nonspecific component of the radioluminescence signal from FM-KIOVs. Thus, the corrected SPR signal corresponding to fluorescein specifically conjugated to cdb3, $L_{cor}^{FM\text{-}cdb3}$, was

$$L_{cor}^{FM\text{-}cdb3} = L_{cor}^{tot} - L_{cor}^{clv} = (S_{bn}^{tot} \cdot I_a^{tot}) - (S_{bn}^{clv} \cdot I_a^{clv}), \quad (4)$$

where the superscripts tot and clv refer to FM-KIOV and clv-FM-KIOV samples, respectively.

SPR distance determination

The distance between the planar distribution of tritium "donors" created by [^{3}H]oleic in the bilayer and the fluorescein "acceptors" conjugated to cdb3 was calculated according to Eq. 5 (Shahrokh et al., 1992):

$$H = [(m\rho_r n_f \Phi)/(L_{cor}^{FM\text{-}cdb3} - b\rho_r n_f \Phi)]^{\xi}, \quad (5)$$

$$\Phi = \sigma_f(Q_y G Q_e),$$

where $L_{cor}^{FM\text{-}cdb3}$ in cps μCi^{-1} [μmol band 3]$^{-1}$ is the inner-filter-corrected SPR signal of cdb3-conjugated fluorescein (from Eq. 4), H is the distance between the fluorophores on cdb3 and the tritium plane in the bilayer (cm), ρ_r is the density of tritium in the bilayer (μCi cm^{-2}), n_f is the number of fluorophores per μmol of band 3, σ_f is the SPR fluorophore cross section ("fraction of exited fluorophores" · cm^3 μCi^{-1} keV^{-1} s^{-1}), Q_y is the fluorophore quantum yield, G is the photon collection efficiency of the ellipsoidal optics, and Q_e is the quantum efficiency of the photomultiplier. The parameters m (1.096×10^{10} keV $cm^{-1+1/\xi}$ μCi^{-1}), b (-2.640×10^{10} keV cm^{-1} μCi^{-1}), and ξ (13.33, dimensionless) were derived from an empirical fit for the range of distances relevant for this study (10–200 Å) to the previously described Monte Carlo simulation relating distance to SPR signal for a point-to-plane geometrical distribution of tritium and fluorophores (Shahrokh et al., 1992). Deviation between Monte Carlo data (obtained every nanometer) and the fitted relationship was under 1%.

The density of tritium in the bilayer (ρ_r) was calculated by assuming 100% [^{3}H]oleic acid incorporation into the bilayer, a red cell surface area of 140 μm^2, and 1.1×10^6 band 3 molecules per cell (Weinstein, 1974; Halestrap, 1976; Funder et al., 1978). Because the calculated distance is strongly dependent on the tritium density (Eq. 5), an attempt was made to select the most probable value for the band 3 quantity, the parameter carrying the largest potential uncertainty. Although estimations of this quantity essentially range between 1.0×10^6 and 1.2×10^6, we based our selection primarily on the direct binding measurements of Funder et al. (1.08×10^6, n = 15) and Halestrap (1.19×10^6, n = 6), which by-passed the uncertainty of membrane protein estimates. Because oleic acid equilibrates rapidly between the two leaflets of the bilayer and because the tritium is located in the middle of the [^{3}H]oleic acid chain, it was assumed that two ^{3}H planes were created, one at the center of each leaflet; the two ^{3}H planes were separated by a half-bilayer thickness, taken as 22 Å. A small correction was needed because of the nonlinear increase in signal between the farther and the closer leaflet. The value of L_{cor} corresponding

to fluorophores located 20–100 Å from a single plane of tritium describing the midplane of the bilayer was compared by computer modeling to that obtained from two equidistant planes of half-tritium density on each side of the bilayer midplane (separated by 22 Å). L_{cor} was multiplied by this correction factor in Eq. 5 when H was calculated, which is the distance between the midplane of the bilayer and the fluorophores. The correction factor was 0.99 for H values close to 60 Å (see Results).

The quantity $\Phi = \sigma_f (Q_y G Q_e)$, which represents the probability for excitation of the acceptor when $Q_y = G = Q_e = 1$, was determined from the simpler expression of the corrected SPR signal, $L'^{FM\text{-}cdb3}_{cor}$, for the case of a random three-dimensional distribution of tritium surrounding the acceptors:

$$L'^{FM\text{-}cdb3}_{cor} = A_r n_f \Phi \langle E \rangle, \quad (6)$$

where A_r is the radioactivity (μCi) from a 1-μCi sample, and $\langle E \rangle = 2.05 \times 10^5$ keV μCi^{-1} cm^{-3} is the weighted mean β-particle energy density per microcurie (Bicknese et al., 1992); this geometrical situation was obtained experimentally with samples in which [^{3}H]oleic acid was replaced by ^3H_2O as the tritium source and nonradioactive oleic acid was substituted for [^{3}H]oleic acid. Use of the same fluoresceinated samples and instrumentation to measure SPR signals in the presence of [^{3}H]oleic acid or ^3H_2O ensured that Φ was equivalent in both geometrical situations. This improved the accuracy of the calculated distance by eliminating the need for independent determination of several peripheral variables (Q_y, G, and Q_e) and reducing the dependence of the distance on other variables.

RET measurements

Fluorescence measurements were carried out on an SLM 8000C fluorimeter (Urbana, IL). Samples were diluted to 9.8 nM band 3 in buffer B, and a quartz cuvette with 10-mm excitation and 2-mm emission pathlengths was used to minimize inner-filter effect and scattering. To minimize direct excitation of the acceptor, excitation wavelengths of fluorescein were 438 and 448 nm for experiments with HAE and ORB, respectively. Emission spectra of samples of FM-KIOVs and clv-FM-KIOVs similarly labeled with the acceptor were recorded in pairs, and these paired measurements repeated for different acceptor densities. Subtraction of instrument-corrected paired spectra yielded the emission spectrum component corresponding to fluorescein specifically conjugated to cdb3 (FM-cdb3) for a given acceptor density. The extent of energy transfer was then determined by the ratio Q_d/Q_{da} of FM-cdb3 fluorescence in the absence and presence of acceptor at 516 nm for HAE, and integrated in the 526–542 nm range for ORB. The fluorescein quantum yield of FM-cdb3 in the absence of acceptor, Q_d, was similarly measured at 438 and 448 nm using free fluorescein in 0.1 M NaOH as standard ($Q = 0.92$). The molar absorbance of FM-cdb3 at 438 and 448 nm was determined by subtracting the absorbance of clv-FM-KIOVs from that of FM-KIOVs (both 98 nM band 3 in buffer B). Absorbance spectra of membrane-incorporated HAE and ORB in buffer B were determined by using acceptor-labeled samples of KIOVs containing 44 nM band 3. Ninety-eight and ninety-nine percent of injected HAE and ORB, respectively, were found to be associated with KIOVs, and these corrections were introduced in the calculation of membrane acceptor densities. From these absorbance spectra and percentage incorporations, maximum molar absorbances of membrane-incorporated acceptor were determined using ϵ_{max} = 110,800 M^{-1} cm^{-1} and ϵ_{max} = 124,800 M^{-1} cm^{-1} for HAE and ORB in methanol (Molecular Probes). The overlap integral J, between the emission of fluorescein on cdb3 and the absorbance of membrane-incorporated HAE or ORB, was calculated by summing Eq. 7 over $\Delta\lambda$ = 1 nm intervals:

$$J = \sum[F_d(\lambda)\, \epsilon_a(\lambda) \lambda^4 \Delta\lambda] / \sum[F_d(\lambda)\Delta\lambda], \quad (7)$$

where λ is the wavelength in nanometers, $F_d(\lambda)$ is the instrument-corrected fluorescence of the donor at λ, and $\epsilon_a(\lambda)$ is the molar absorbance in M^{-1} cm^{-1} of the acceptor at λ.

The donor-acceptor Förster distance, R_0 (in Å), was calculated from Eq. 8 (Wu and Brand, 1994):

$$R_0(Å) = (8.785 \times 10^{-5}\, J\, \kappa^2 Q_d n^{-4})^{1/6}, \quad (8)$$

where n is the refractive index of the buffer (Moog et al., 1984) (taken as 1.34) and κ^2 is the orientation factor for dipole-dipole transfer (taken as 2/3). κ^2 = 2/3 only when donors and acceptors either rotate freely during a time that is short relative to the excited lifetime of the donor or are isotropically distributed (Dale and Eisinger, 1974; Stryer, 1978); such was not the case here, and the value of κ^2 could theoretically range from 0 to 4. However, because the above conditions were partially met, the range of possible κ^2 values could be narrowed (Dale et al., 1979) by using the fluorescence depolarization factor of the fluorescein donor, which was previously shown to wobble rapidly within a cone of 44° semiangle at pH 7.4 (Thevenin et al., 1994), and by exploiting the random distribution of the acceptor dipole moments of HAE and ORB in the membrane (Holowka and Baird, 1983; Fung and Stryer, 1978). For this situation where the donor had freedom of reorientation over the volume of a 44° cone and acceptor orientations were isotropically distributed, minimum (0.47) and maximum (1.07) values for κ^2 were determined from figure 20 in Dale and Eisinger (1974). These extreme κ^2 values were then incorporated into Eq. 8 to calculate the maximum and minimum R_0 values for each donor-acceptor pair.

RET distance determination

Protein crowding of the erythrocyte bilayer by large intramembrane particles (e.g., band 3 dimers) complicates the determination of the separation between a point fluorescein donor beneath the membrane and a plane of lipid acceptors in the bilayer. This is because acceptors are excluded from a substantial area of the membrane and the distribution of acceptors in the plane of the bilayer cannot be assumed to be uniform. To correct formally for the exclusion of lipids by proteins, a numerical modeling of RET efficiencies between donor fluorophores located on intramembrane particles crowding the bilayer and acceptor probes distributed in this bilayer was developed using Monte Carlo simulations of membrane particle distributions (Zimet et al., 1995). The specific model of the erythrocyte membrane used here assumed that fluorescent donors were positioned on the rotational axis of randomly distributed incompressible disks representing intramembranous band 3 particles, and that acceptor lipid fluorophores were randomly distributed around the area occupied by band 3 particles and formed a single acceptor plane. The particle density was taken as 0.55×10^6 band 3 dimers per cell (or 140-μm^2 membrane area), and the diameter of the lipid disk excluded by each particle was assumed to be 90 Å. The total fraction of lipid-excluded membrane surface was therefore 25%, in accord with reported values (Saxton, 1989). Random donor protein coordinate sets and acceptor coordinate sets were generated for these conditions and used to calculate Q_{da}/Q_d for distances ranging between 0 and 60 Å and for normalized acceptor densities (acceptor/R_0^2) ranging between 0 and 1, as described (Zimet et al., 1995). Because the diameter of the lipid-excluded particle disk is a parameter normalized to R_0, these calculations were repeated for each R_0 value of the two fluorescent pairs as well as for each of their minimum and maximum values.

RESULTS

Stoichiometric labeling of band 3 Cys-201 with fluorescein

Fig. 2 *A* shows the labeling specificity of the band 3 Cys-cluster in KIOVs with fluorescein maleimide under conditions that label Cys-201, the most reactive of the two clustered cysteines from each cdb3 subunit (Thevenin et al., 1989). Predominant labeling of band 3 in KIOVs is shown in Lane 1. Lane 2 shows that band 3 was exclusively labeled

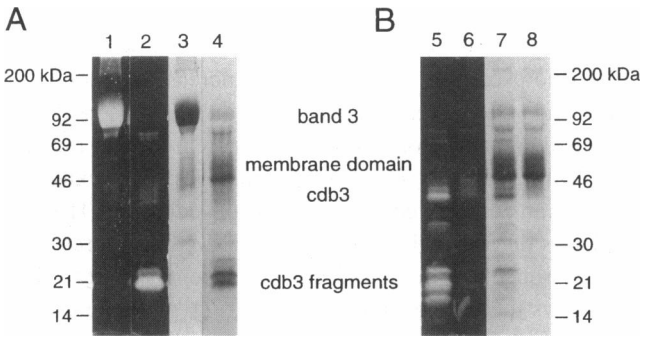

FIGURE 2 (*A*) Stoichiometric labeling of band 3 Cys-201 in KIOVs with fluorescein maleimide (see Materials and Methods). Lanes 1 and 3, FM-KIOVs; Lanes 2 and 4, FM-KIOVs cleaved at 1 mg/ml with 1 μg/ml trypsin for 30 min at 0°C. Lanes 1 and 2, Fluorescence profile; Lanes 3 and 4, Coomassie staining profile. The electrophoretic mobilities of both 20-kDa C-terminal and 21-kDa N-terminal fragments are anomalously low. The minor fluorescent band above the main labeled 20-kDa band in Lane 2 is distinct from the N-terminal 21-kDa fragment and represents a larger form of the C-terminal fragment, which can be further cleaved into the 20-kDa fragment. (*B*) Chymotryptic cleavage and removal of cdb3 from FM-KIOVs (see Materials and Methods). Lanes 5 and 7, FM-KIOVs cleaved with chymotrypsin but unwashed; Lanes 6 and 8, equivalent amounts (in terms of membrane surface area) of chymotrypsin-cleaved FM-KIOVs after washing out cdb3 fragments (clv-FM-KIOVs); Lanes 5 and 6, fluorescence profile; Lanes 7 and 8, Coomassie staining profile.

in the C-terminal 20-kDa segment of its cytoplasmic domain, which contains the Cys-cluster. Stoichiometric labeling of each cdb3 was indicated from the electrophoretic mobility of the 20-kDa tryptic fragment of band 3, which is further reduced by each fluorescein conjugation (Thevenin et al., 1994). Stoichiometric labeling of cdb3 was confirmed by direct measurement of the difference in labeling between FM-KIOVs before and after chymotryptic removal of cdb3, which was found to be 1.1 mol fluorescein/mol of band 3 monomer. Fig. 2 *B* shows the fluorescence and Coomassie staining profiles of FM-KIOVs after chymotryptic cleavage but before removal of cdb3 fragments (Lanes 5 and 7) and of clv-FM-KIOVs (after removal of cdb3 fragments; Lanes 6 and 8). These samples contained equivalent amounts of the 55-kDa membrane domain of band 3, which was the criterion used to establish equivalency in membrane surface area between samples of clv-FM-KIOVs and FM-KIOVs.

Determination of the Cys-201:bilayer distance by SPR

To determine the distance between the bilayer and fluorescein conjugated to cdb3, radioluminescence of fluorescein was measured in the presence of [9,10(n)-^{3}H]oleic acid incorporated into the bilayer of FM-KIOVs and clv-FM-KIOVs as tritium donors. The measured radioluminescence signals contained a background signal that was independent of the fluorescein or tritium content of these doubly labeled samples and measured to be ~10 cps using FM-KIOV, clv-FM-KIOV, and KIOV samples labeled with nonradioactive oleic acid (Table 1). This background level was

TABLE 1 Summary of SPR measurements

	FM-KIOVs	clv-FM-KIOVs	KIOVs (*Bremsstrahlung*)	FM-cdb3
[^{3}H]Oleic acid	85.3 ± 1.2	41.5 ± 0.2	17.0 ± 0.4	98.5 ± 2.1
^3H_2O	36.6 ± 0.3	21.0 ± 0.9	ND	38.4 ± 1.6

Background-corrected, normalized SPR signals obtained with the various KIOV samples in the presence of [^{3}H]oleic acid or ^3H_2O are given as mean ± SD cps μCi^{-1} [μmol band 3]$^{-1}$ of triplicate determinations (c.f. S_{bn} signals in Materials and Methods). The instrument background signals measured with FM-KIOV, clv-FM-KIOV, and KIOV samples labeled with nonradioactive oleic acid were 10.1 ± 0.4, 10.8 ± 0.8, and 10.1 ± 0.3 cps, respectively. The background signal constituted ~8% of the total signal from FM-KIOVs with [^{3}H]oleic acid. The *Bremsstrahlung* component of S_{bn} signals (see text), determined with tritiated but unfluoresceinated KIOV samples, is also reported. ND, Not determined. Shown in the last column are the corrected SPR signals of fluorescein conjugated to cdb3 ($L_{cor}^{FM\text{-}cdb3}$) obtained from the difference in inner-filter-corrected S_{bn} signals between FM-KIOVs and clv-FM-KIOVs (Eq. 4); inner-filter correction factors for the FM-KIOV and clv-FM-KIOV samples were calculated from Eq. 3 to be 1.75 and 1.22, respectively.

similar to instrument noise obtained with the shutter closed (~9 cps) and indicated the absence of phosphorescence and chemiluminescence from the vials and the samples. After subtraction of the background signal, the measured SPR signals from the doubly labeled samples were normalized for tritium radioactivity and sample quantity (Eq. 1). These background-subtracted normalized signals (S_{bn}) are reported in Table 1. These signals contained a radioactivity-dependent component corresponding to photons generated by *Bremsstrahlung* or "stopping radiation" (Bicknese et al., 1992). This component was measured using tritiated nonfluorescent KIOVs and amounted to ~20% of S_{bn} from doubly labeled FM-KIOVs (Table 1). Correcting S_{bn} for inner-filter effect and subtracting the *Bremsstrahlung* component yielded the corrected SPR signal, L_{cor} (Eq. 2). L_{cor} corresponding exclusively to cdb3-conjugated fluorescein was determined by subtracting the inner-filter-corrected S_{bn} of clv-FM-KIOVs from that of FM-KIOVs, because both contained the same *Bremsstrahlung* component (Eq. 4). The corrected radioluminescence produced by excitation of fluorescein specifically conjugated to cdb3 (FM-cdb3) by [^{3}H]oleic acid was $L_{cor}^{FM\text{-}cdb3} = 98.5 \pm 2.1$ cps μCi^{-1} [μmol band 3]$^{-1}$ (Table 1).

To calculate the distance between the plane of tritium donors and fluorescein acceptors corresponding to this corrected SPR signal from FM-cdb3 in the presence of [^{3}H]oleic acid, it was necessary to determine Φ, the cross section of FM-cdb3 for excitation by tritium as defined in Eq. 5. Φ was measured using samples in which ^3H_2O replaced [^{3}H]oleic acid as the tritium source (Eq. 6). These samples preserved the geometrical characteristics of the fluorescein acceptor while creating a random three-dimensional distribution of tritium. The corrected SPR signal from FM-cdb3 in the presence of ^3H_2O, $L'^{FM\text{-}cdb3}_{cor}$, was obtained by subtracting the inner-filter-corrected S_{bn} of clv-FM-KIOVs from that of FM-KIOVs (Table 1). $L'^{FM\text{-}cdb3}_{cor}$ was measured as 38.4 ± 1.6 cps μCi^{-1} [μmol band 3]$^{-1}$, and Φ

was calculated to be $(2.82 \pm 1.2) \times 10^{-22}$ "fraction of excited fluorophores" $\cdot$ cm^3 μCi^{-1} keV^{-1} s^{-1} for FM-cdb3. Correcting $L_{cor}^{FM\text{-}cdb3}$ obtained with [^{3}H]oleic acid for the biplanar distribution of tritium in the bilayer (see Materials and Methods), the separation between the midplane of the bilayer and fluorescein on cdb3 was calculated from Eq. 5 to be 61 $\pm$ 7 Å (mean $\pm$ SD, when accounting for SDs from all measured variables). A graphic determination is shown in Fig. 3, which presents the relationship between the SPR signal for a point-to-plane geometrical distribution of tritium and fluorophores as a function of the point-to-plane separation, and from which Eq. 5 was derived. After subtracting 22 Å for the half-bilayer thickness, the distance between Cys-201 of band 3 and the surface of the bilayer was 39 $\pm$ 7 Å.

Determination of the Cys-201:bilayer distance by RET

To measure the distance between Cys-201 and the bilayer by RET, fluorescein linked to Cys-201 of cdb3 was used as the "donor" fluorophore and lipid probes were introduced in the bilayer as the "acceptor." Two different lipid acceptors were used, HAE, an anionic probe, and ORB, a cationic probe. Fluorescence emission spectra corresponding to fluorescein specifically conjugated to cdb3 (FM-cdb3) were obtained in the presence of various acceptor concentrations by subtracting the emission spectrum of each acceptor-labeled sample of clv-FM-KIOVs from that of a sample of FM-KIOVs identically labeled with acceptors. Fig. 4, *A* and *B*, shows the cdb3-specific component of the emission spectra of fluorescein in the presence of increasing amounts of HAE and ORB, respectively. Donor fluorescence was quenched and acceptor fluorescence increased with increasing acceptor density (sensitized emission). The extent of energy transfer between fluorescein on cdb3 and HAE or ORB was determined as the ratio of FM-cdb3 fluorescence in the absence and in the presence of acceptor, Q_d/Q_{da}. Fig. 4 *C* shows the relationship between Q_d/Q_{da} and the density of HAE and ORB in the membrane.

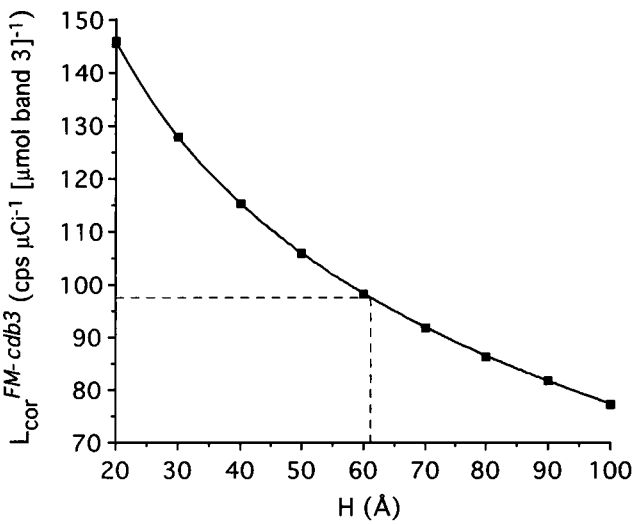

FIGURE 3 Relationship between the corrected SPR signal for fluorescein on cdb3 ($L_{cor}^{FM\text{-}cdb3}$) and the fluorophore-tritium distance (H), as derived from a Monte Carlo simulation relating SPR signal and the separation between fluorophore and tritium in a point-to-plane geometry (see Eq. 5). The value of Φ is given in the text, ρ_r was 9.20×10^{-5} μCi cm^{-2}, and n_f was 6.64×10^{17} (μmol band 3)$^{-1}$. The value of $L_{cor}^{FM\text{-}cdb3}$ from Table 1 was multiplied by 0.99 to correct for the biplanar distribution of tritium in the two leaflets (see Materials and Methods). The graphical determination yields H = 61 Å, which gives a Cys-201:bilayer distance of 39 Å after subtraction of 22 Å for the half-bilayer thickness.

The relationship between energy transfer efficiency, $1 - Q_{da}/Q_d$, and the distance H from donor fluorophores to a uniform planar distribution of acceptors can be approximated by a linear function (Yguerabide, 1994). However, the assumption of uniformity in the planar distribution of lipid acceptors is invalid for the erythrocyte membrane because of the substantial size and abundance of band 3 particles. The expression of RET was therefore derived numerically by modeling RET efficiencies between a fluorescent donor on a membrane protein and acceptors distributed in a protein-crowded membrane using a separately described Monte Carlo approach (Zimet et al., 1995). Specifically, RET efficiencies for the erythrocyte membrane situation were calculated for each relevant Förster distance, R_0, by modeling the bilayer as containing a total lipid-excluded area of 25% contributed by randomly distributed band 3 dimers (see Materials and Methods). R_0 values were determined to be 57 Å for the FM-cdb3:HAE pair and 56 Å for the FM-cdb3:ORB pair.

As shown in Fig. 5 *A*, calculations of RET in the case of an R_0 of 56 Å and a fixed distance between donor and acceptor plane of H = 42 Å yielded a nearly linear relationship between Q_d/Q_{da} and the acceptor density. This was also the case when the calculations were carried out with an R_0 of 57 Å (not shown). These results were in agreement with the experimental findings presented in Fig. 4 *C*, provided that $H \approx 42$ Å (see below). Linear relationships between Q_d/Q_{da} and the density of HAE and ORB were therefore assumed with respective slopes of 34.7 and 28.5 nm^2/acceptor. The numerical modeling of RET was also used to derive the relationship between Q_d/Q_{da} and H for a given R_0 value. Fig. 5 *B* shows the distance dependency of Q_d/Q_{da} for an R_0 value of 56 Å and an acceptor density = $0.6\ R_0^{-2}$. The distance H between fluorescein donors on cdb3 and the crowded acceptor plane was determined from the calculated relationships to be 40 and 43 Å for the acceptors HAE and ORB, respectively. These distances represent the separation between Cys-201, the labeling site on cdb3, and the surface of the membrane, because the fluorophores HAE and ORB do not equilibrate between leaflets and their fluorescent headgroups distribute at the surface of the bilayer. Primary parameters and results of this measurement of the Cys-201:bilayer distance by RET are summarized in Table 2.

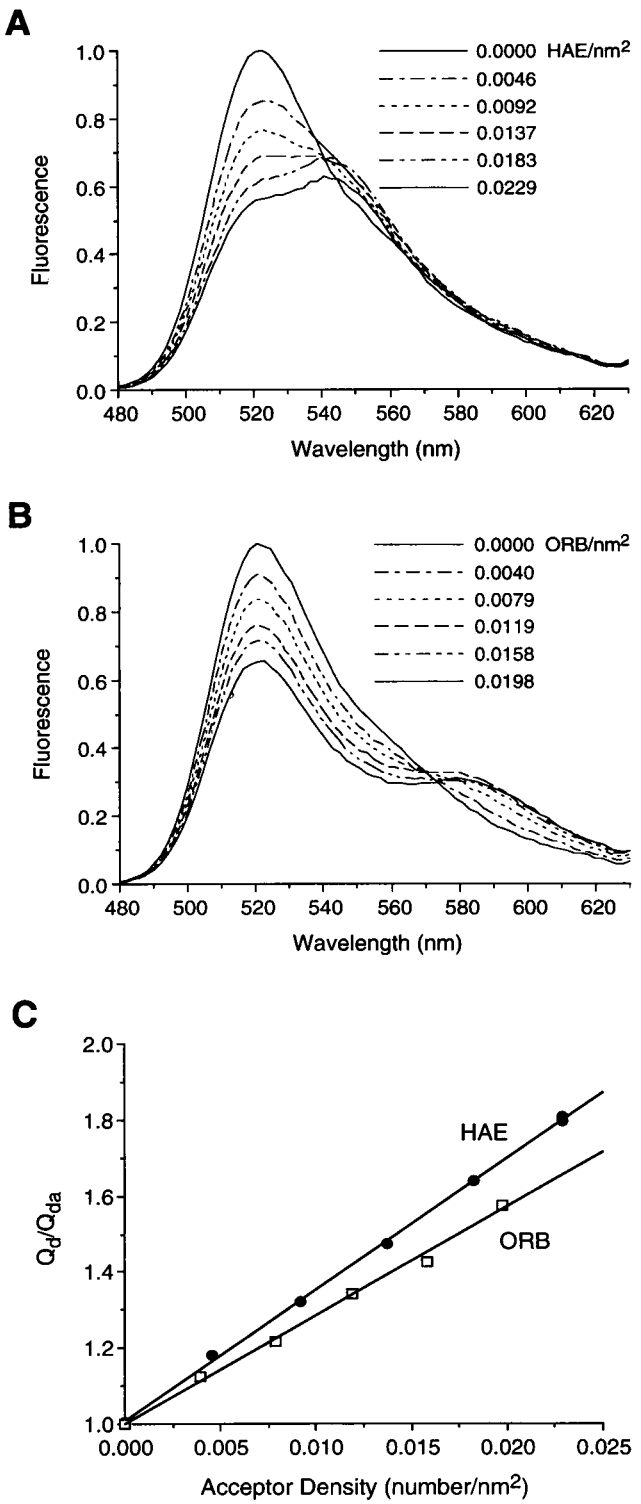

FIGURE 4 RET between Cys-201 and the bilayer. (*A* and *B*) Emission spectra of fluorescein on cdb3 in the presence of increasing membrane densities of HAE and ORB, respectively. Spectra were obtained by subtracting the emission of clv-FM-KIOVs from that of FM-KIOVs for each acceptor density. Spectra shown are uncorrected for inner filter effect and are taken from a representative RET experiment. (*C*) Ratio of donor fluorescence in the absence and in the presence of acceptor, Q_d/Q_{da}, at increasing acceptor density. A small correction for inner filter effect (0.55% and 0.32% at the highest density of HAE and ORB) was applied to these ratios.

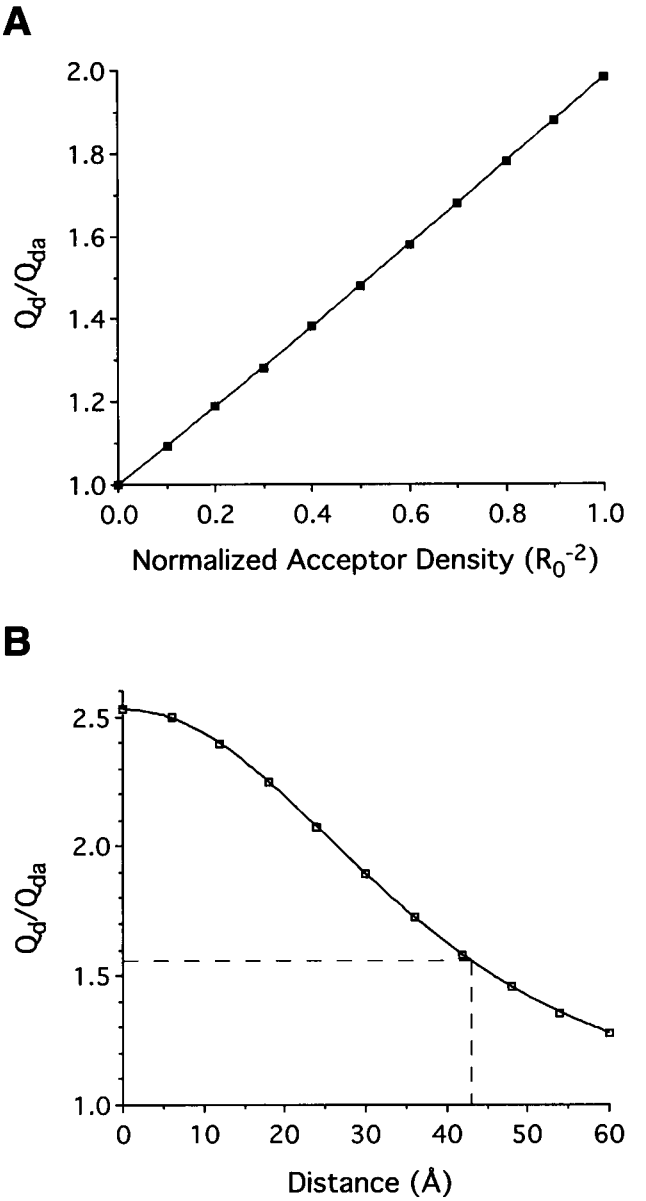

FIGURE 5 Results obtained by numerical modeling of RET in the erythrocyte membrane. The bilayer was assumed to be crowded by randomly distributed band 3 dimers 90 Å in diameter contributing to a total lipid-excluded membrane surface of 25% (see Materials and Methods). R_0 was 56 Å, the R_0 of the fluorescein-ORB pair. (*A*) Calculated Q_d/Q_{da} between point donors and the acceptor plane separated by H = 42 Å as a function of acceptor density. (*B*) Calculated relationship between Q_d/Q_{da} and the distance H for a lipid density of 0.6 R_0^{-2}. For this density of ORB (0.0191 nm^{-2}), Q_d/Q_{da} = 1.56; the corresponding distance is determined to be 43 Å.

DISCUSSION

SPR utilizes the energy deposited by low-energy β-particles from a tritium source to excite nearby acceptor fluorophores (Bicknese et al., 1992). Because the energy deposited into the surrounding medium falls off with distance, SPR is suitable for the study of molecular distances on a submicron scale (Shahrokh et al., 1992). SPR has been applied to

TABLE 2 Summary of RET measurements

Donor	λ_{Em} (nm)	Q	$r_{\infty f}$	Acceptor	λ_{Abs} (nm)	ε_{max} ($M^{-1} \cdot cm^{-1}$)	J ($M^{-1} \cdot cm^{-1} \cdot nm^4$)	R_0 (Å)	Max. range R_0 (Å)	Slope Q_d/Q_{da} vs acceptor density (nm^2/acceptor)	H (Å)	Max. range H (Å)
FM-cdb3	521	0.53	0.15	HAE	528	96,000	3.66×10^{15}	57	54–62	34.7	40	34–48
FM-cdb3	521	0.53	0.15	ORB	563	95,700	3.25×10^{15}	56	53–61	28.5	43	37–51

FM-cdb3 parameters were obtained by subtraction of clv-FM-KIOV spectral data from that of FM-KIOVs. $r_{\infty f}$ is the previously measured limiting anisotropy associated with the fast component of the time-resolved anisotropy of FM-KIOVs at pH 7.4 (Thevenin et al., 1994). The steady-state anisotropy of fluorescein maleimide labeled cdb3 was also measured as 0.15 at pH 7.4. The slope of Q_d/Q_{da} versus acceptor density was obtained from the data in Fig. 4 *C*, assuming linearity (see text). The maximum range of R_0 was calculated using minimum and maximum κ^2 values (0.47 and 1.07), and it was then used to determine the maximum range of H values (see Materials and Methods).

several studies of relative proximity, including ligand binding, lipid exchange kinetics, membrane transport, and investigation of tryptophan environment (Shahrokh et al., 1992; Bicknese et al., 1995). In addition, an averaged separation between the erythrocyte bilayer and bound wheat germ agglutinin was determined (Shahrokh et al., 1992). However, quantitative submicron distance information provided by SPR has not been confirmed by an independent method. This report describes the application of SPR to the determination of an absolute molecular distance related to the structure of a major membrane protein, erythrocyte band 3, and its independent measurement by RET. The distance between Cys-201 of the cytoplasmic sulfhydryl cluster of band 3 and the surface of the bilayer was measured by both SPR and RET. Cys-201 was labeled with fluorescein maleimide, whereas the bilayer was labeled with [^{3}H]oleic acid as the tritium source for SPR measurements or with HAE and ORB as acceptors for RET measurements. The two independent techniques yielded Cys-201:bilayer distance values that were in agreement (~40 Å).

Crowding effects

Distance determinations by RET between a point donor positioned on a membrane protein and a planar distribution of acceptors in the bilayer have generally assumed that acceptors were uniformly distributed. However, this approximation is invalid in the case of the Cys-201:bilayer distance, because the size of the lipid area excluded by each band 3 particle is not small in comparison, and the erythrocyte membrane is substantially crowded by band 3 proteins (Saxton, 1989). A few studies have employed analytical approximations to correct for the presence of the donor protein, but these did not account for the presence of the other intramembrane proteins (Fleming et al., 1979; Kleinfeld and Lukacovic, 1985; Stefanova et al., 1993; Corbalan-Garcia et al., 1993; Valenzuela et al., 1994). To correct for the exclusion of lipid acceptors by both the protein bearing the donor and other particles, RET efficiencies were numerically calculated using Monte Carlo-generated random distributions of band 3 particles and surrounding lipid acceptors. Band 3 particles were assumed to be randomly distributed dimers excluding acceptors from a 90-Å-diameter disk, as inferred from electron micrographs of the membrane (Weinstein et al., 1978). Although the cross section of band 3 dimers through the cytoplasmic side of the bilayer is now believed to be elliptical (60 × 110 Å; Wang et al., 1994), inclusion of this geometry for the lipid area excluded by band 3 would not substantially alter calculated RET efficiencies. Furthermore, this small potential effect on the distance is counterweighted by not having considered that ~30% of band 3 may be present as tetramers rather than as dimers (Casey and Reithmeier, 1991). The separation between Cys-201 and the bilayer was calculated to be ~41 Å, ~21 Å less than the distance obtained when neglecting the presence of band 3. This result demonstrates that the error from overlooking protein crowding in biological membranes can be substantial.

Orientational uncertainty

RET is sensitive to the relative orientation of the donor and acceptor transition moments during the dipole-dipole energy transfer process, which is described by the orientation factor κ^2. Because κ^2 is typically unknown, distances are calculated assuming dynamic averaging, $\kappa^2 = 2/3$. Fortunately, the degree of orientational freedom of fluorophores in biological samples as measured by their fluorescence depolarization narrows the theoretical range of κ^2 values (Dale et al., 1979), and the 1/6 power dependence of the Förster distance R_0 on κ^2 further minimizes the uncertainty (Stryer, 1978). The rapid wobbling of fluorescein conjugated to cdb3 Cys-201 has been identified by time-resolved anisotropy (Thevenin et al., 1994). In addition, the isotropic distribution of the fluorophores on the lipid probes HAE and ORB has been inferred from RET studies (Holowka and Baird 83, Fung and Stryer 78). Under these conditions, the maximum uncertainty in R_0 was calculated to be ~7% and corresponded to a maximum error of ~7 Å in the measured distance (Table 2). This uncertainty would be further reduced by taking into account the nanosecond segmental motion of the portion of band 3 bearing the fluorescein label (Thevenin et al., 1994) and the substantial motion of the acceptor fluorophore inferred from steady-state depolarization measurements (Holowka and Baird, 1983; Isaacs et al., 1986; Carraway et al., 1990). Importantly, the close agreement between the 40- and 43-Å distances measured with different acceptors of opposite charge further validates the

assumption $\kappa^2 = 2/3$ (Stryer, 1978). It is therefore unlikely that the orientation factor introduced any substantial error into our measurements.

Comparisons between SPR and RET

There are several differences between the measurement of molecular distances by SPR and RET. First, radioluminescence is unaffected by the orientation of the fluorophore and would be useful to determine distances when the anisotropy of the fluorophores exceeds 0.3 and the uncertainty from the orientation factor becomes unacceptable. Second, SPR is relatively insensitive to the presence of proteins in the bilayer because β-particles deposit their energy along tortuous paths that are very long compared to the size of the membrane proteins, so that the lost contribution from a lipid-excluded area to the total energy deposited in a given location is small. Third, SPR allows distances to be measured from a site that can be tritiated when introduction of a fluorescent label would alter the structure of the substrate. Fourth, SPR is unaffected by sample turbidity, which can limit RET measurements in membranes or other highly scattering samples. Last and most importantly, radioluminescence is suitable for distance determinations in the 10–1000-Å range, which encompasses both molecular and intracellular distances. Thus SPR not only is a suitable alternative to RET in many cases, but may also be the only satisfactory technique for distance determinations in a number of specialized situations.

When comparing SPR with RET for the measurement of distances in biological samples, it is important to note the greater theoretical dependency of the SPR distance on several experimental or instrument parameters (compare Eq. 5 and Eq. 8). In practice, however, this potential source of inaccuracy can be greatly minimized when additional measurements are possible with a modified sample in which the relative position of tritium donors and acceptor fluorophores is known. As was done in this study, the easiest method to create a geometrically defined arrangement of tritium and fluorophores while preserving all other sample characteristics is to substitute ^3H_2O as the tritium source because it produces a uniform distribution of tritium around the acceptor. With this maneuver, distance becomes solely dependent on tritium densities and inner-filter-corrected SPR signals (with the inner-filter correction having very limited weight), and the experimental protocol for distance measurement by SPR becomes simpler than that with RET, which typically involves multiple peripheral determinations. A practical limitation in the use of SPR is the requirement for relatively large amounts of fluorescent sample (nmol/sample) and radioactivity (10–100 μCi/sample). In addition, switching tritium and acceptor positions when measuring distances from a membrane is not possible because of the "scintillant" effect of the bilayer on the SPR fluorophore cross section (Bicknese et al., 1992). Finally, a theoretical weakness of SPR is its inability to resolve multiple distinct distances (for example, due to labeling or conformational heterogeneity), which is possible by RET using multicomponent lifetime analysis (Bigelow and Inesi, 1993; Wu and Brand, 1994).

Implications for the structure of band 3

The binding sites for the disulfonate stilbene (DS) family of anion exchange inhibitors have received considerable attention to structure and mechanism. Nevertheless, information regarding the location of these inhibitory sites within the membrane domain of band 3 has been limited to the findings that, even though labeled from the outside, DS sites must reside at some depth inside the membrane (Rao et al., 1979; Eidelman et al., 1991) and that the two DS sites of a band 3 dimer are separated by at least 28 Å (Macara and Cantley, 1981; Wojcicki and Beth, 1993). In their RET study, Rao et al. (1979) found by lifetime analysis that the two DS sites were at similar distances from the Cys-cluster and made multiple measurements of the distance between the DS site and the cytoplasmic cysteines, which ranged from 37 to 47 Å.* This distance is very similar to the separation measured here between the Cys-cluster and the inner surface of the bilayer. Thus the DS sites and the inner surface are at nearly the same distance from the Cys-cluster. This extends the previous conclusion that the DS site was deep within the membrane, by indicating that it is very close to the cytoplasmic surface of the bilayer.

Insight into the orientation of cdb3 in the membrane is also provided by the approximate equidistance of the bilayer and the DS sites from the Cys-cluster. Let us assume that the two DS sites of a band 3 dimer are located in the plane of the cytoplasmic surface of the bilayer, separated by at least 28 Å, and equidistant from the vertical rotational axis of band 3. Let us also assume that the four cysteines in the dimer, which lie within a few Å of each other, describe a single locus. In one extreme situation, this locus could be in the plane that is perpendicular to the bilayer and equidistant from the two DS sites. In this situation, even when using the longest measured distance between the Cys-cluster and the DS sites (47 Å) and the shortest measured separation between the Cys-cluster and the bilayer (39 Å), the longest distance from the Cys-cluster to the rotational axis of band 3 is calculated by triangulation to be 22 Å. Alternatively, the Cys-cluster could be in the plane that is perpendicular to the bilayer but contains the two DS sites. In this case, the separation between the Cys-cluster and the rotational axis of band 3 also cannot exceed 22 Å, because the distances from the Cys-cluster to each of the two DS sites would be

*The distance values between DS sites and the Cys-cluster obtained by Rao et al. (1979), using multiple probes and exchanging the location of donors and acceptors to improve accuracy, were recalculated assuming the most probable model for RET: each Cys probe on cdb3 interacted equally with two DS acceptors in a band 3 dimer and each DS donor interacted equally with up to four Cys probes on a cdb3 dimer. The same refractive index value as in the present study was used.

different enough or long enough to contradict the RET findings of Rao et al. (1979). It can be similarly established that the maximum distance between the Cys-cluster and the rotational axis of band 3 is not able to exceed 22 Å in all situations intermediate between these two extreme examples. Thus this proximity of the Cys-cluster to the vertical rotational axis of band 3 suggests that the orientation of the C-terminal subdomain of cdb3 extending from the membrane is nearly perpendicular to the bilayer.

Hydrodynamic properties of isolated cdb3 have implied considerable asymmetry and led to the previous estimation that the domain's structure extends ~250 Å with an axial ratio of 10 (Low, 1986). To achieve this length both segments on either side of the central hinge in cdb3, the 20-kDa C-terminal subdomain above the hinge and the 21-kDa N-terminal subdomain below the hinge, have been assumed to be highly extended. However, the present finding that the position of band 3 Cys-201, only 10 residues away from the hinge, is ~40 Å from the bilayer and close to the rotational axis, indicates that cdb3 is not substantially elongated between the membrane and the hinge. For example, even if the two C-terminal subdomains of cdb3 were packed into a cylinder extending from the membrane as far as 50 Å, its diameter would still be calculated to exceed 35 Å. This conclusion allows us to provide in Fig. 6 a revised working diagram of the structure of band 3 with a compact arrangement between the membrane and the hinge. This unextended structure of the C-terminal subdomains of cdb3 does not preclude substantial asymmetry of its N-terminal subdomains and therefore of the entire cdb3. However, the relatively short span of the C-terminal "half" of cdb3 makes it very unlikely that the overall length of cdb3 would reach even 200 Å. Because the estimate of a 250 Å length was highly dependent on the assumption of a cylindrical shape for cdb3, the present result may indicate that cdb3 in the membrane cannot be approximated by a cylinder. For example, an inverted Y or an asymmetrical X shape for the cdb3 dimer might better explain the present finding in light of the high frictional ratio of isolated cdb3.

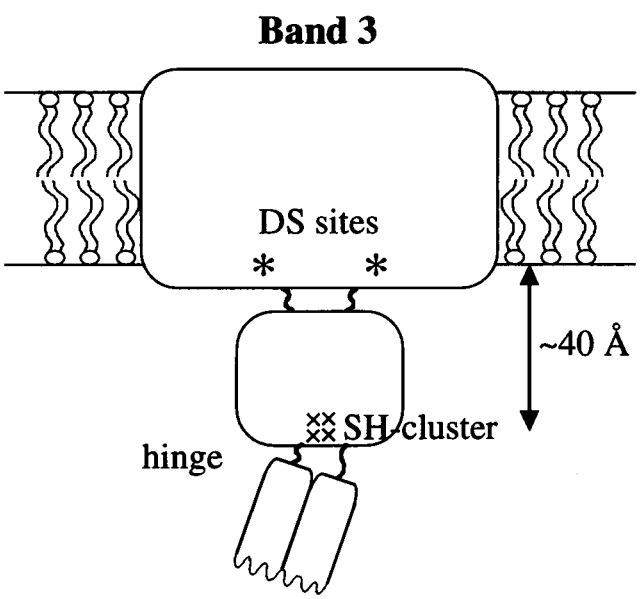

FIGURE 6 Diagram of band 3, showing the proposed arrangement of cdb3 between the hinge and the membrane. The portion of cdb3 C-terminal of the hinge is connected to the membrane domain via two flexible stretches. The two subunits comprising this portion of cdb3 are arranged in a compact configuration which, if roughly cylindrical with a length of ~35 Å, would have a diameter of least 45 Å. The two DS inhibitory sites are shown aligned with the inner surface of the bilayer, and the approximate positions of the four cytoplasmic cysteines ~40 Å from the bilayer and close to the rotational axis of band 3 are indicated. The arrangement of cdb3 on the N-terminal side of the hinge is unknown, and its partial representation is arbitrary.

The authors gratefully acknowledge the technical assistance of Mr. Julius Park during SPR measurements.

This work was supported by grant BE 229 from the American Cancer Society, grants DK16095 and DK43480 from the National Institute of Health, and a grant-in-aid from the W. Duncan MacMillan Trust.

REFERENCES

Agre, P., E. P. Orringer, D. H. K. Chui, and V. Bennett. 1981. A molecular defect in two families with hemolytic poikilocytic anemia. *J. Clin. Invest.* 68:1566–1576.

Bennett, V. 1983. Proteins involved in membrane-cytoskeleton associations in human erythrocytes: spectrin, ankyrin, and band 3. *Methods Enzymol.* 96:313–324.

Bicknese, S. E., Z. Shahrokh, S. B. Shohet, and A. S. Verkman. 1992. Single photon radioluminescence. I. Theory and spectroscopic properties. *Biophys. J.* 63:1256–1266.

Bicknese, S. E., D. B. Zimet, J. Park, A. N. van Hoek, S. B. Shohet, and A. S. Verkman. 1995. Detection of water proximity to tryptophan residues in protein by single photon radioluminescence. *Biophys. Chem.* 54:279–290.

Bigelow, D. J., and G. Inesi. 1991. Frequency-domain fluorescence spectroscopy resolves the location of maleimide-directed spectroscopic probes within the tertiary structure of the Ca-ATPase of sarcoplasmic reticulum. *Biochemistry.* 30:2113–2125.

Carraway, K. L., III, J. G. Koland, and R. A. Cerione. 1990. Location of the epidermal growth factor binding site on the EGF receptor. A resonance energy transfer study. *Biochemistry.* 29:8741–8747.

Casey, J. R., and R. A. F. Reithmeier. 1991. Analysis of the oligomeric state of band 3, the anion transport protein of the human erythrocyte membrane, by size exclusion high performance liquid chromatography. Oligomeric stability and origin of heterogeneity. *J. Biol. Chem.* 266: 15726–15737.

Corbalan-Garcia, S., J. A. Teruel, and J. C. Gomez-Fernandez. 1993. Intramolecular distances within the Ca^{2+}-ATPase from sarcoplasmic reticulum as estimated through fluorescence energy transfer between probes. *Eur. J. Biochem.* 217:737–744.

Dale, R. E., and J. Eisinger. 1974. Intramolecular distances determined by energy transfer. Dependence on orientational freedom of donor and acceptor. *Biopolymers.* 13:1573–1605.

Dale, R. E., J. Eisinger, and W. E. Blumberg. 1979. The orientational freedom of molecular probes. The orientation factor in intramolecular energy transfer. *Biophys. J.* 26:161–194.

Eidelman, O., P. Yanai, H. C. Englert, H. G. Lang, R. Greger, and Z. I. Cabantchik. 1991. Macromolecular conjugates of transport inhibitors: new tools for probing topography of anion transport proteins. *Am. J. Physiol.* 260:C1094–C1103.

Fleming, P. J., D. E. Koppel, A. L. Y. Lau, and P. Strittmatter. 1979. Intramembrane position of the fluorescent tryptophanyl residue in membrane-bound cytochrome b_5. *Biochemistry.* 18:5458–5464.

Funder, J., D. C. Tosteson, and J. O. Wieth. 1978. Effects of bicarbonate on lithium transport in human red cells. *J. Gen. Physiol.* 71:721–746.

Fung, B. K.-K., and L. Stryer. 1978. Surface density determination in membranes by fluorescence energy transfer. *Biochemistry.* 17: 5241–5248.

Halestrap, A. P. 1976. Transport of pyruvate and lactate into human erythrocytes. *Biochem. J.* 156:193–207.

Holowka, D., and B. Baird. 1983. Structural studies on the membrane-bound immunoglobulin E-receptor complex. 1. Characterization of large plasma membrane vesicles from rat basophilic leukemia cells and insertion of amphipathic fluorescent probes. *Biochemistry.* 22:3466–3474.

Isaacs, B. S., E. J. Husten, C. T. Esmon, and A. E. Johnson. 1986. A domain of membrane-bound blood coagulation factor Va is located far from the phospholipid surface. A fluorescence energy transfer measurement. *Biochemistry.* 25:4958–4969.

Jennings, M. L. 1989. Structure and function of the red blood cell anion transport protein. *Annu. Rev. Biophys. Biophys. Chem.* 18:397–430.

Kleinfeld, A. M., and M. F. Lukacovic. 1985. Energy-transfer study of cytochrome b_5 using the anthroyloxy fatty acid membrane probes. *Biochemistry.* 24:1883–1890.

Low, P. S. 1986. Structure and function of the cytoplasmic domain of band 3: center of erythrocyte membrane-peripheral protein interactions. *Biochim. Biophys. Acta.* 864:145–167.

Low, P. S., M. A. Westfall, D. P. Allen, and K. C. Appell. 1984. Characterization of the reversible conformational equilibrium of the cytoplasmic domain of erythrocyte membrane band 3. *J. Biol. Chem.* 259: 13070–13076.

Low, P. S., B. M. Willardson, N. Mohandas, M. Rossi, and S. B. Shohet. 1991. Contribution of the band 3-ankyrin interaction to erythrocyte membrane mechanical stability. *Blood.* 77:1581–1586.

Lowry, O. H., N. J. Rosebrough, A. L. Farr, and R. J. Randall. 1951. Protein measurement with the Folin phenol reagent. *J. Biol. Chem.* 193:265–275.

Macara, I. G., and L. C. Cantley. 1981. Interactions between transport inhibitors at the anion binding sites of the band 3 dimer. *Biochemistry.* 20:5095–5105.

Moog, R. S., A. Kuki, M. D. Fayer, and S. G. Boxer. 1984. Excitation transport and trapping in a synthetic chlorophyllide substituted hemoglobin: orientation of the chlorophyll S1 transition dipole. *Biochemistry.* 23:1564–1571.

Peters, L. L., and S. E. Lux. 1993. Ankyrins: structure and function in normal cells and hereditary spherocytes. *Semin. Hematol.* 30:85–118.

Rao, A., P. Martin, R. A. F. Reithmeier, and L. C. Cantley. 1979. Location of the stilbenedisulfonate binding site of the human erythrocyte anion-exchange system by resonance energy transfer. *Biochemistry.* 18: 4505–4516.

Reithmeier, R. A. F. 1993. The erythrocyte anion transporter (band 3). *Curr. Opin. Struct. Biol.* 3:515–523.

Salhany, J. M., and R. Cassoly. 1989. Kinetics of *p*-mercuribenzoate binding to sulfhydryl groups on the isolated cytoplasmic fragment of band 3 protein. Effect of hemoglobin binding on the conformation. *J. Biol. Chem.* 264:1399–1404.

Saxton, M. J. 1989. Lateral diffusion in an archipelago. Distance dependence of the diffusion coefficient. *Biophys. J.* 56:615–622.

Shahrokh, Z., S. E. Bicknese, S. B. Shohet, and A. S. Verkman. 1992. Single photon radioluminescence. II. Signal detection and biological applications. *Biophys. J.* 63:1267–1279.

Stefanova, H. I., A. M. Mata, M. G. Gore, J. M. East, and A. G. Lee. 1993. Labeling the (Ca^{2+}-Mg^{2+})-ATPase of sarcoplasmic reticulum at GPu-439 with 5-(bromo methyl) fluorescein. *Biochemistry.* 32:6095–6103.

Stryer, L. 1978. Fluorescence energy transfer as a spectroscopic ruler. *Annu. Rev. Biochem.* 47:819–846.

Tanner, M. J. A. 1993. Molecular and cellular biology of the erythrocyte anion exchanger (AE1). *Semin. Hematol.* 30:34–57.

Tanner, M. J. A., P. G. Martin, and S. High. 1988. The complete amino acid sequence of the human erythrocyte membrane anion-transport protein deduced from the cDNA sequence. *Biochem. J.* 256:703–712.

Thevenin, B. J.-M., and P. S. Low. 1990. Kinetics and regulation of the ankyrin-band 3 interaction of the human red blood cell membrane. *J. Biol. Chem.* 265:16166–16172.

Thevenin, B. J.-M., N. Periasamy, S. B. Shohet, and A. S. Verkman. 1994. Segmental dynamics of the cytoplasmic domain of erythrocyte band 3 determined by time-resolved fluorescence anisotropy: sensitivity to pH and ligand binding. *Proc. Natl. Acad. Sci. USA.* 91:1741–1745.

Thevenin, B. J.-M., B. M. Willardson, and P. S. Low. 1989. The redox state of cysteines 201 and 317 of the erythrocyte anion exchanger is critical for ankyrin binding. *J. Biol. Chem.* 264:15886–15892.

Valenzuela, C. F., P. Weign, J. Yguerabide, and D. A. Johnson. 1994. Transverse distance between the membrane and the agonist binding sites on the *Torpedo* acetylcholine receptor: a fluorescence study. *Biophys. J.* 66:674–682.

Wang, D. N., V. E. Sarabia, R. A. F. Reithmeier, and W. Kühlbrandt. 1994. Three dimensional map of the dimeric membrane domain of the erythrocyte anion exchanger, band 3. *EMBO J.* 13:3230–3235.

Weinstein, R. S. 1974. The morphology of adult red cells. *In* The Red Blood Cell. D. M. Surgenor, editor. Academic Press, New York. 213–268.

Weinstein, R. S., J. K. Khodadad, and T. L. Steck. 1978. Fine structure of the band 3 protein in the human red cell membrane: freeze-fracture studies. *J. Supramol. Struct.* 8:325–335.

Willardson, B. M., B. J.-M. Thevenin, M. L. Harrison, W. M. Kuster, M. D. Benson, and P. S. Low. 1989. Localization of the ankyrin-binding site on erythrocyte membrane protein, band 3. *J. Biol. Chem.* 264: 15893–15899.

Wojcicki, W. E., and A. H. Beth. 1993. Structural and binding properties of the stilbenedisulfonate sites on erythrocyte band 3: an electron paramagnetic resonance study using spin-labeled stilbenedisulfonates. *Biochemistry.* 32:9454–9464.

Wu, P., and L. Brand. 1994. Resonance energy transfer: methods and applications. *Anal. Biochem.* 218:1–13.

Yguerabide, J. 1994. Theory for establishing proximity relations in biological membranes by excitation energy transfer measurements. *Biophys. J.* 66:683–693.

Zimet, D. B., B. J.-M. Thevenin, A. S. Verkman, S. B. Shohet, and J. R. Abney. 1995. Calculation of resonance energy transfer in crowded biological membranes. *Biophys. J.* 68:1592–1603.